

Nucleon flow and fragment flow in heavy ion reactions

Akira Ono, Hisashi Horiuchi, and Toshiki Maruyama*

Department of Physics, Kyoto University, Kyoto 606-01, Japan

(Received 2 August 1993)

The collective flow of nucleons and that of fragments in the $^{12}\text{C} + ^{12}\text{C}$ reaction below 150 MeV/nucleon are calculated with the antisymmetrized version of molecular dynamics combined with the statistical decay calculation. The density dependent Gogny force is used as the effective interaction. The calculated balance energy is about 100 MeV/nucleon, which is close to the observed value. Below the balance energy, the absolute value of the fragment flow is larger than that of nucleon flow, which is also in accordance with data. The dependence of the flow on the stochastic collision cross section and its origin are discussed. All the results are naturally understood by introducing the concept of two components of flow: the flow of dynamically emitted nucleons and the flow of the nuclear matter which contributes to both the flow of fragments and the flow of nucleons due to the statistical decay.

PACS number(s): 25.70.-z, 21.65.+f, 24.10.Cn

I. INTRODUCTION

The collective flow in heavy ion reactions in the intermediate and high energy regions has been studied both experimentally and theoretically with the expectation that it carries the information of hot and dense nuclear matter. However, by studying with microscopic simulation approaches, such as the Vlasov-Uehling-Uhlenbeck (VUU) method, it has turned out that extracting the equation of state from the collective flow is not easy since it reflects not only the equation of state but also the cross section of the two-nucleon collision term which has theoretical ambiguity in the nuclear medium.

Although the collective flow is a one-body observable, the most characteristic feature of intermediate energy heavy ion reactions is the fragment formation. Recently the collective flow has been measured with the identification of charges and/or mass numbers of fragments [1,2]. The large flow of fragments is observed compared to the flow of nucleons, which suggests that the flow of composite fragments carries the direct information of the equation of state (or the mean field), while most nucleons are emitted by the hard stochastic collisions which erase the effect of the mean field. Thus we can expect that the study of the fragment flow together with the nucleon flow may give us important information on the equation of state.

For the theoretical analysis of the flow of fragments, the model should be able to describe the dynamical fragment formation, and we use the antisymmetrized version of molecular dynamics (AMD) [3-5] which was constructed by incorporating the stochastic collision process into the fermionic molecular dynamics that describes the

system with a Slater determinant of Gaussian wave packets [6-8]. We have demonstrated that the AMD can describe some quantum mechanical features such as the shell effect in the cross sections of the dynamical production of the fragments. Since the flow of α particles is important among the flows of various fragments, this ability of the AMD to describe the large cross sections of the dynamical production of α particles is a very advantageous property of the AMD for the present study. Furthermore, AMD has an advantage that the calculation with finite-range effective interaction is as feasible as the calculation with zero-range effective interaction, and therefore the momentum dependence of the mean field, which is essential for the study of the equation of state, is automatically taken into the calculation.

In studying the collective flow, we should also pay attention to the momentum distribution of the produced fragments. Namely, since the flow is known to be a very sensitive quantity to the various parameters in the theory, such dependence should be understood on the level of the momentum distribution. For example, some change of the equation of state and another change of the in-medium cross section may result in the same change of the flow value, but this does not mean that one must give up the determination of the equation of state by using heavy ion reactions. We still have a chance that these two changes will result in the distinguishable changes of the momentum distribution of fragments. Our framework AMD is suitable for study of the momentum distribution of fragments since there is no ambiguity in identifying the fragments. As we pointed out in Ref. [5], the dissipated component of the momentum distribution of fragments such as α particles is sensitive to the in-medium cross section, while the flow angle is expected to be sensitive to the effective interaction.

In this paper, we will investigate the flow of nucleons and fragments for the reaction $^{12}\text{C} + ^{12}\text{C}$ in the energy regions $45 \text{ MeV/nucleon} \leq E \leq 150 \text{ MeV/nucleon}$ which includes the observed balance energy. After giving a brief explanation of our framework in Sec. II, we discuss in Sec.

*Present address: Advanced Science Research Center, Japan Atomic Energy Research Institute, Tokai-mura, Ibaraki-ken 319-11, Japan.

III the use of the finite range Gogny force [9] as the effective interaction which gives the soft equation of state with the incompressibility of the nuclear matter $K = 228$ MeV. It is shown that the Gogny force reproduces binding energies of light nuclei relevant to the present study. In Sec. IV, before showing the calculated results of the flow, we will check the validity of our calculation by comparing the proton spectra with the data and the results of other calculations. In Sec. V, the calculated results of the flow are shown and it will turn out that the soft equation of state with the Gogny force is consistent to the experimentally observed balance energy of the flow. The calculated flow of α particles is larger than the flow of nucleons, which is also consistent with the feature of the experimental data, and the mechanism of the creation of these flows will be revealed by paying attention to the time scale of the reaction and dividing the collective flow into two components, i.e., the flow of dynamically emitted nucleons and the flow of the nuclear matter. In Sec. VI, the dependence of the flow on the in-medium cross section and the origin of this dependence are discussed. Sec. VII is devoted to the summary.

II. FRAMEWORK

Since the framework of the antisymmetrized version of molecular dynamics (AMD) was described in detail in Refs. [4,5], here we show only the outline of our framework.

In AMD, the wave function of the A -nucleon system $|\Phi\rangle$ is described by a Slater determinant $|\Phi(\mathbf{Z})\rangle$,

$$|\Phi(\mathbf{Z})\rangle = \frac{1}{\sqrt{A!}} \det[\varphi_i(j)], \quad \varphi_i = \phi_{\mathbf{z}_i} \chi_{\alpha_i}, \quad (1)$$

where α_i represents the spin-isospin label of the i th single-particle state, $\alpha_i = p \uparrow, p \downarrow, n \uparrow, \text{ or } n \downarrow$, and χ is the spin-isospin wave function. $\phi_{\mathbf{z}_i}$ is the spatial wave function of the i th single-particle state which is a Gaussian wave packet

$$\langle \mathbf{r} | \phi_{\mathbf{z}_i} \rangle = \left(\frac{2\nu}{\pi} \right)^{3/4} \exp \left[-\nu \left(\mathbf{r} - \frac{\mathbf{Z}_i}{\sqrt{\nu}} \right)^2 + \frac{1}{2} \mathbf{Z}_i^2 \right], \quad (2)$$

where the width parameter ν is treated as time-independent in our model. We took $\nu = 0.16 \text{ fm}^{-2}$ in the calculation presented in this paper.

The time developments of the centers of Gaussian wave packets, $\{\mathbf{Z}_i (i = 1, 2, \dots, A)\}$, are determined by two processes. One is the time development determined by the time-dependent variational principle

$$\delta \int_{t_1}^{t_2} dt \frac{\langle \Phi(\mathbf{Z}) | (i\hbar \frac{d}{dt} - H) | \Phi(\mathbf{Z}) \rangle}{\langle \Phi(\mathbf{Z}) | \Phi(\mathbf{Z}) \rangle} = 0, \quad (3)$$

which leads to the equation of motion for $\{\mathbf{Z}\}$.

The second process which determines the time development of the system is the stochastic collision process due to the residual interaction. We incorporate this process in a similar way to the quantum molecular dynam-

ics (QMD) by introducing the physical coordinates $\{\mathbf{W}_i\}$ [3,4] as

$$\mathbf{W}_i = \sum_{j=1}^A \left(\sqrt{Q} \right)_{ij} \mathbf{Z}_j, \quad (4)$$

where

$$Q_{ij} = \frac{\partial}{\partial (\mathbf{Z}_i^* \cdot \mathbf{Z}_j)} \ln \langle \Phi(\mathbf{Z}) | \Phi(\mathbf{Z}) \rangle. \quad (5)$$

In addition to the usual two nucleon collision process, the stochastic nucleon-alpha collision process is also included as in Ref. [5]. Since we apply AMD to the reactions with higher incident energy in this paper than in the previous works [3–5], the cross sections and the angular distributions of the stochastic collisions are reparametrized as explained in Appendix B.

Since in AMD the center-of-mass motion of the fragment is described by the Gaussian wave packet, we have to subtract from the AMD Hamiltonian $\langle \Phi(\mathbf{Z}) | H | \Phi(\mathbf{Z}) \rangle / \langle \Phi(\mathbf{Z}) | \Phi(\mathbf{Z}) \rangle$ the sum of the spurious zero-point energies of the fragments whose number changes in time. The prescription to deal with this problem which is a revised version of the previous prescription in Refs. [3–5] is explained in Appendix C.

The simulations of AMD are truncated at a finite time (150 fm/c in the calculation presented in this paper). The dynamical stage of the reaction has finished by this time and some excited fragments have been formed which will emit lighter particles with a long time scale. Such statistical decays of the equilibrated fragments are calculated with a code of Ref. [10] which is similar to the code of Pühlhofer [11].

III. CHOICE OF THE EFFECTIVE INTERACTION

Since the collective flow is expected to reflect the momentum dependence and the density dependence of the mean field, the choice of the effective interaction in our framework is important.

The momentum dependence of the mean field can be taken into account as long as a finite range effective interaction is used, since the system is described with an antisymmetrized wave function in AMD. The calculation with a finite range force is as feasible as the calculation with a zero-range force in AMD, and therefore we have been using finite range effective interactions. In Refs. [3–5] we used the Volkov force No. 1 [12] with the Majorana parameter $m = 0.576$, which is a density-independent two-range interaction. By adjusting the parameter related to the subtraction of the spurious zero-point oscillation of fragments, the binding energies of nuclei lighter than ^{12}C are reproduced very well. However, heavier nuclei are overbinding with this effective interaction as shown in Fig. 1. When the Volkov force is applied, usually its Majorana parameter m should be chosen depending on the mass number of the nuclei under consid-

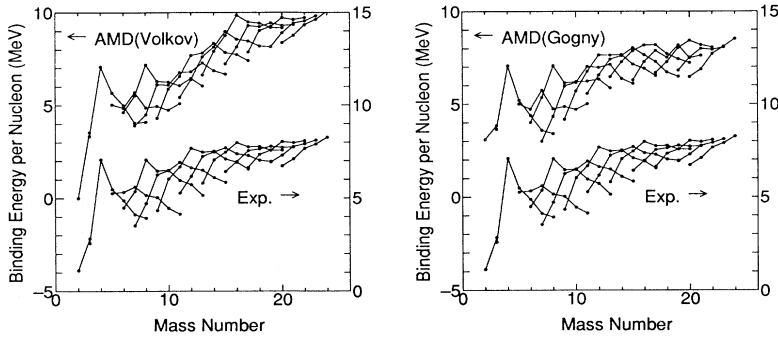


FIG. 1. Binding energies per nucleon of nuclei calculated with the Volkov force No. 1 ($m = 0.576$) (left) and the Gogny force (right). Isotopes are connected with lines. Experimental data shifted by -5 MeV are also shown.

eration, which makes the Volkov force very inconvenient for our study.

In order to reproduce the binding energies of nuclei in wide mass number region within a single effective interaction, and in order to cope duely with the formation of the high density nuclear matter in collisions with high incident energy around and above 100 MeV/nucleon, the density dependence of the effective interaction should be introduced. We use the Gogny force [9] in the calculation presented in this paper. The binding energies of nuclei lighter than ^{24}Mg are reproduced (Fig. 1) by adjusting the parameter related to the subtraction of the spurious zero-point oscillation of fragments which is described in Appendix C. It is known that the Gogny force can describe the saturation property of nuclear matter with the incompressibility $K = 228$ MeV. The momentum dependence of the mean field with the Gogny force is reliable below 200 MeV, since the energy dependence of the real part of the nucleon optical potential is reproduced in this energy range. The Gogny force has been successfully applied to the problem of the flow in the framework of VUU [13].

The calculation with density dependent zero-range force requires us to evaluate the quantities such as

$$\int d\mathbf{r} \rho(\mathbf{r})^{2+\sigma}, \quad (6)$$

where $\rho(\mathbf{r})$ is the density calculated with the AMD wave function. This spatial integration was performed by a kind of Monte Carlo method with test particles generated randomly with a weight function. The detail of the calculation method is explained in Appendix A. If we use 100A test particles, the statistical error in the evaluation of the energy of ^{12}C ground state is about 2 MeV, which seems sufficiently small for the current purpose.

IV. ENERGY SPECTRA OF PROTONS

Before going into the problem of the collective flow, we compare our results on the proton energy spectrum to the data in the $^{12}\text{C} + ^{12}\text{C}$ reaction at the incident energy 84 MeV/nucleon, which was also analyzed by other simulation methods such as VUU and QMD [14]. It is for the purpose of showing the reliability of the AMD calculation in the incident energy region around 100 MeV/nucleon.

As mentioned before [3–5], the AMD has proved to be very successful in reproducing the nuclide distribution and the fragment energy spectra in the incident energy region around the Fermi energy.

In Fig. 2, the calculated proton energy spectra for various angles are compared to the data [15]. The dotted histograms are the calculated proton spectra at the end of AMD simulation $t = 150$ fm/c, which do not contain the contribution from the statistical decay of excited fragments after $t = 150$ fm/c, while the solid histograms are the final results which should be compared to the data. We can see that the effect of the statistical decay of fragments on these spectra is not so large except for the low energy part. Although our calculation has a tendency to overestimate the proton spectra at 35° – 65° , this feature and the degree of the overestimation are common with other simulation approaches such as VUU and QMD [14]. The spectra of backward angles are reproduced by our model as well as by QMD. In Fig. 3, the multiplicity of nucleons are shown as a function of the impact param-

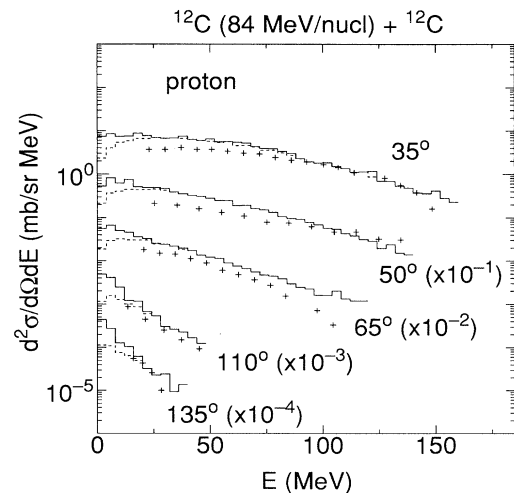


FIG. 2. Energy spectra of protons for the reaction $^{12}\text{C} + ^{12}\text{C}$ at 84 MeV/nucleon. Dashed histograms are the proton spectra calculated before the statistical decay, the solid histograms are the final calculated results. Experimental data are shown by crosses. Energy E and angles are in the laboratory system.

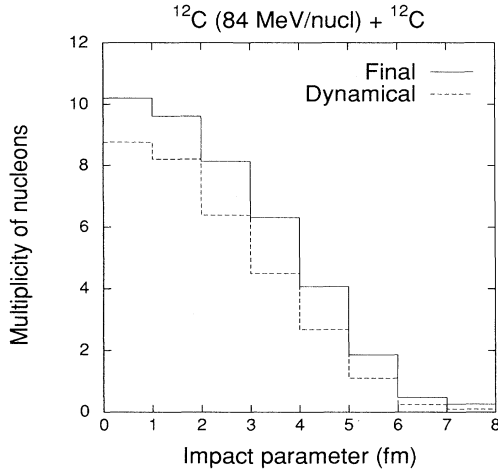


FIG. 3. Impact parameter dependence of the nucleon multiplicity for the reaction $^{12}\text{C} + ^{12}\text{C}$ at 84 MeV/nucleon. Dashed histogram shows the multiplicity before the statistical decay and the solid histogram shows the final calculated result.

eter. The dynamical contribution before the statistical decay is shown as well as the final multiplicity. This result is again quite similar to those of QMD and VUU [14] for all the impact parameter regions.

In calculating the spectra in our model, we must attribute some widths to the momenta of nucleons and fragments produced in the AMD calculation, since these momenta are central values of Gaussian wave packets. Each wave packet has the width $\Delta p/\sqrt{A_F}$ in the momentum per nucleon where $\Delta p = \hbar\sqrt{\nu}$ and A_F is the mass number of the fragment. However, we should not always take this width to have physical meaning, since some part of this width comes from the unphysical width of the projectile or the target in the initial state of the simulation. It seems reasonable to consider that such unphysical contribution mainly goes to the momentum widths of fragments and to assume that all the widths of the wave packets of nucleons are physical. When the proton spectra in Fig. 2 are calculated, we neglect the widths of the fragments produced dynamically in the AMD simulation, but attribute the widths to the dynamically produced nucleons in the AMD simulation.

V. CALCULATED RESULTS OF THE FLOW AND THE MECHANISM OF THE FLOW CREATION

Although the definition of the flow is somewhat complicated in the experimental situation where the determination of the reaction plane is not trivial, we simply define here the flow of fragments with mass number A_F as the mean in-plane transverse momentum,

$$\langle wP_x \rangle / A_F, \quad (7)$$

where $w = 1$ if $P_z > 0$ and $w = -1$ if $P_z < 0$. P_x and P_z are the components of the in-plane momentum

of the fragment in the center-of-mass system which are perpendicular to and along with the beam direction, respectively. Negative flow corresponds to the attractive interaction between the projectile and the target. This definition of the flow was already used in Ref. [16] and has almost no uncertainty due to the interpretation of the momentum width of the wave packets discussed in the previous section.

Another definition of the flow as the slope of $\langle P_x \rangle - P_z$ curve is of course possible, but we have checked that the qualitative features to be discussed below do not change. The statistical precision of the flow defined by Eq. (7) is better than the latter one.

Figure 4 shows the energy dependence of the calculated flows of nucleons and α particles. In this figure, as well as in all the results hereafter, the impact parameter of the reaction is fixed to be 2 fm in order to improve the statistical precision. We can see that the calculated flows of nucleons and α particles change their sign at the balance energy $E_{\text{bal}} = (100 \pm 20)$ MeV, though the balance energy of α particles seems to be larger than that of nucleons. This calculated balance energy is not different so much from the experimentally deduced value 122 ± 12 MeV/nucleon [2]. On the other hand, in the calculation with the Volkov force, the flows of nucleons and α particles are negative even at the incident energy 150 MeV/nucleon [17]. (In this calculation, another version of the stochastic collision process adopted in Ref. [5] was used.)

A remarkable feature is that the absolute value of the flow of α particles is much larger than that of nucleons in the energy region $E < E_{\text{bal}}$. The reason for this larger flow of fragments becomes clear by distinguishing nucleons and fragments according to the time they are produced. We can see from Fig. 5, which shows the distribution of the emission time of nucleons, that the dynamical stage of the reaction has already finished at $t = 150$ fm/c. Figure 6 shows the flows at $t = 150$ fm/c (dynamical) and the flows of nucleons and α particles which are pro-

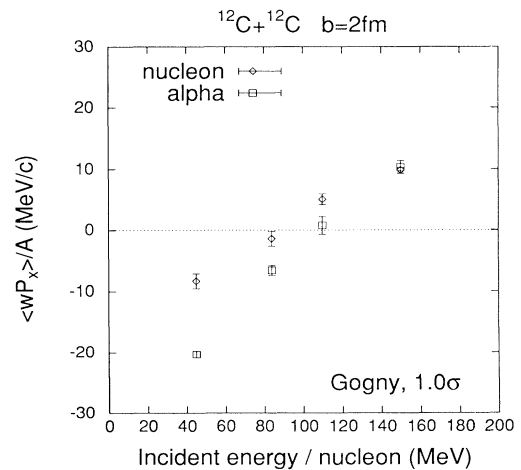


FIG. 4. Calculated flows of nucleons and α particles for various incident energies for the reaction $^{12}\text{C} + ^{12}\text{C}$. The impact parameter of the simulation is fixed to be 2 fm.

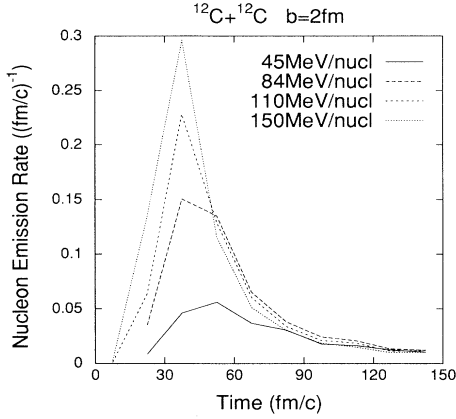


FIG. 5. Time dependence of the nucleon emission rate for the central reaction $^{12}\text{C} + ^{12}\text{C}$ ($b = 2$ fm) at various incident energies. A nucleon is interpreted to have been emitted when no other nucleons exist within a radius of 3 fm.

duced by the statistical decay of other fragments after $t = 150$ fm/c (evaporation). Although the “dynamical” flows in the figure contain some contribution from the equilibrated stage of the reaction, we can see a clear difference between the flow of dynamically emitted nucleons and the flow of evaporated nucleons from the equilibrated fragments. The negative flow of the evaporated nucleons is much larger than the flow of the dynamically emitted nucleons, and the final result is between them. Since a larger number of nucleons are emitted in the dynamical stage, as can be seen from Fig. 7, the final result is closer to the flow of the dynamically emitted nucleons. On the other hand, the flow of α particles seems to be almost independent of the time they are produced, and the value of the flow is close to the flow of the evaporated nucleons.

These results lead us almost uniquely to the following interpretation. We can separate the collective flow into two components. The first one is the flow of the nucleons which are emitted by the hard stochastic colli-

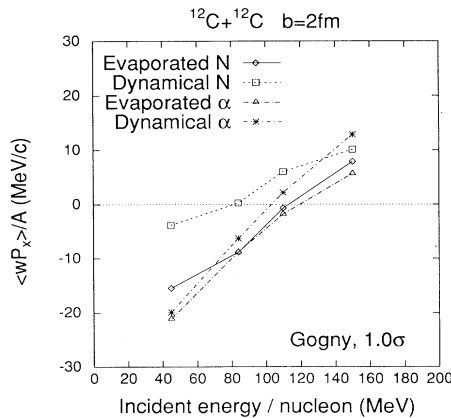


FIG. 6. The dynamical flows of nucleons and α particles which are calculated before the statistical decay, and the flows of evaporated particles which are calculated only from the decay products of the statistical decay.

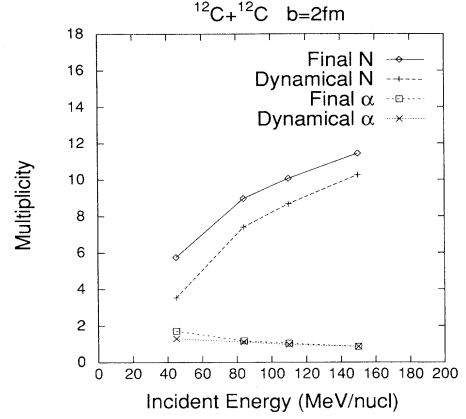


FIG. 7. Incident energy dependence of the multiplicities of nucleons and α particles for the reaction $^{12}\text{C} + ^{12}\text{C}$ with $b = 2$ fm. It is to be noted that some of dynamical α particles decay in the long time scale.

sions in the dynamical stage of the reaction. Since the stochastic collision erases the memory of the mean field, which the nucleon has been feeling before it is scattered, the absolute value of the negative flow is small. There may be another geometrical reason for this small flow: the projectile and the target prevent the nucleons with negative flow from going out to the free space more than the nucleons with positive flow. The second component of the collective flow is the flow of the nuclear matter which contributes to the flows of composite fragments produced in the dynamical stage of the reaction. This component has been affected directly by the mean field and the absolute value of the negative flow is large. The flows of evaporated nucleons and fragments inherit the flow of the parent fragments and hence they have the large value similar to the original nuclear matter flow.

VI. DEPENDENCE ON THE STOCHASTIC COLLISION CROSS SECTION

Since the stochastic collision cross sections have some theoretical uncertainty, we should investigate the dependence of the flow on them. Furthermore, the study of such σ dependence of the momentum distribution will give us the way to determine the in-medium cross sections.

Figures 8 and 9 show the σ dependence of the flows of nucleons and α particles at the incident energy 45 MeV/nucleon and 110 MeV/nucleon, respectively, when all the cross sections (see Appendix B) are multiplied by 0.5, 1.0, and 1.5. The flows of the dynamically produced particles and the flows of the particles produced by the statistical decay are shown together with the final results. The flow of the dynamically emitted nucleons is almost independent of the cross sections. The multiplicity of dynamically emitted nucleons in the reaction at 45 MeV/nucleon is 2.00, 3.52, and 4.95 for 0.5σ , 1.0σ and 1.5σ , respectively. These results are consistent with the

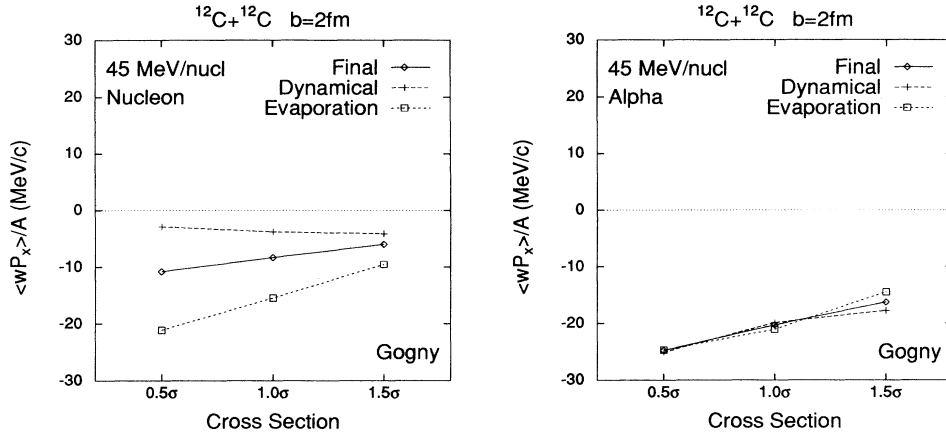


FIG. 8. Dependence of the flows on the stochastic collision cross sections for the reaction $^{12}\text{C} + ^{12}\text{C}$ at 45 MeV/nucleon.

interpretation in the previous section because what is important to the flow of the dynamically emitted nucleons is that the emitted nucleons are direct products of the stochastic collisions and the number of such nucleons is not relevant to the value of the flow.

On the other hand, the σ dependence of the flow of the nuclear matter is large, especially in the reaction at 45 MeV/nucleon, and the absolute value of the negative flow is smaller for larger cross sections. This might sound inconsistent to the naive expectation from the previous interpretation that the flow of the matter is essentially affected by the mean field. This σ dependence, however, turns out to be very reasonable when one pays attention to other features of the momentum distribution as well as the flow. Figures 10 and 11 show the in-plane momentum distribution of nucleons and α particles which are calculated at $t = 150$ fm/c (dynamical) and from those produced by the statistical decay process (evaporation), respectively. Results for three cross sections 0.5σ , 1.0σ , and 1.5σ are shown for the reaction at 45 MeV/nucleon. The momentum distribution of dynamically emitted nucleons is almost spherical while the other three momentum distributions (of evaporated nucleons, dynamical α particles, and evaporated α particles) have the common σ dependence though the momentum distribution of the evaporated nucleons has wider spreading compared to

that of α particles. As the cross sections are increased, the dissipated component of the momentum distribution around the center-of-mass momentum increases while the flow angle does not change. What has changed the flow value of the matter is nothing but this σ dependence of the dissipated component of the momentum distribution.

It is to be noted here that the σ dependence of the flow is not due to the specific definition of the flow (7). For example, if we adopt the definition of the flow as the slope of $\langle P_x \rangle - P_z$ curve at $P_z = 0$, we get the σ dependence of the nucleon flow shown in Fig. 12 which has the same qualitative feature as the left part of Fig. 8.

VII. SUMMARY

In this paper the collective flow of fragments was calculated as well as the flow of nucleons with the AMD for the reaction $^{12}\text{C} + ^{12}\text{C}$ in the energy range 45 MeV/nucleon $\leq E \leq 150$ MeV/nucleon. The balance energy observed in the experiment was found to be consistent with the Gogny force which yields a soft equation of state with $K = 228$ MeV. We obtained a larger absolute value of the fragment flow than the nucleon flow, which is also consistent with the experimentally observed feature.

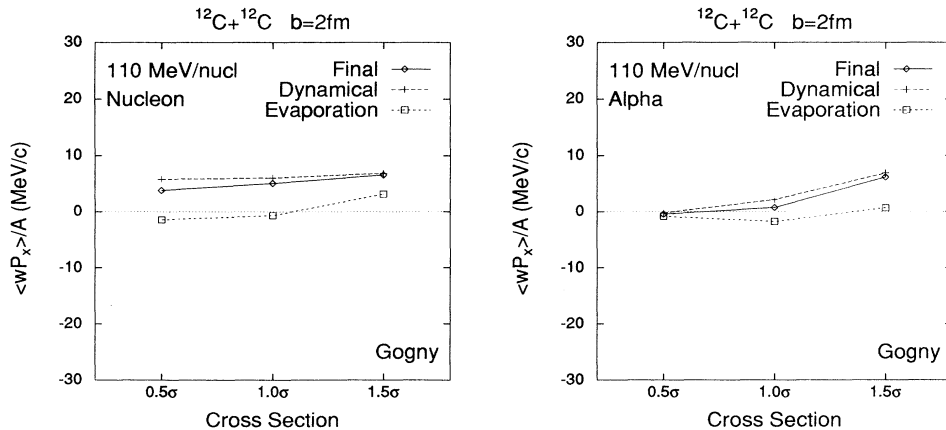


FIG. 9. Dependence of the flows on the stochastic collision cross sections for the reaction $^{12}\text{C} + ^{12}\text{C}$ at 110 MeV/nucleon.

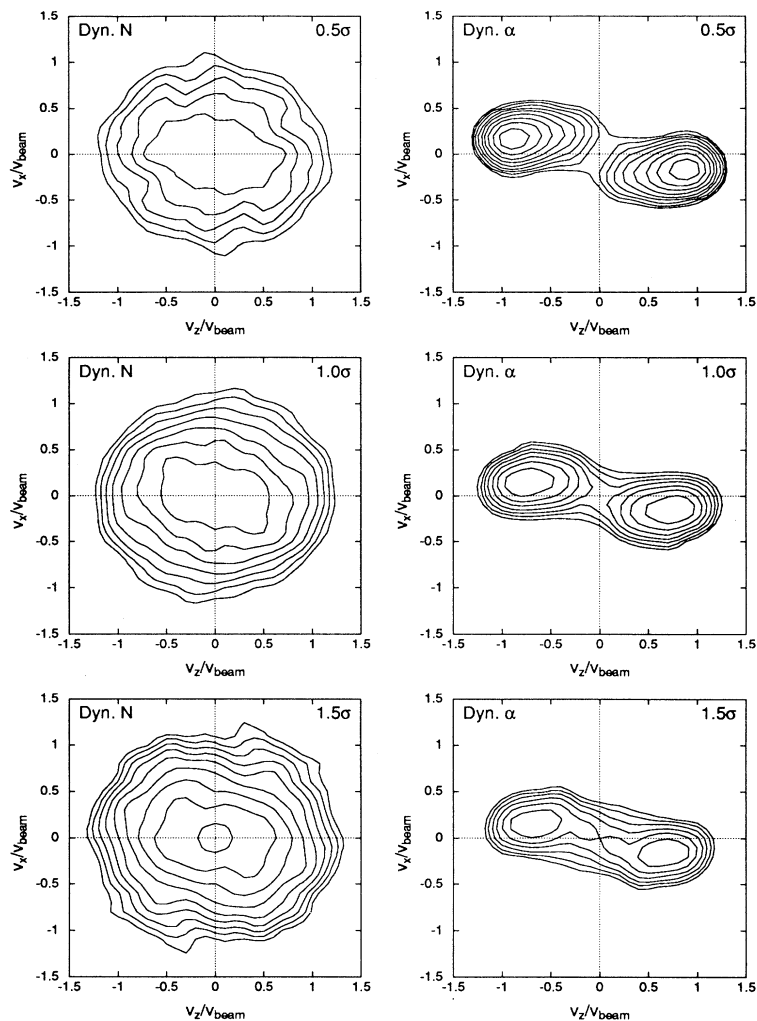


FIG. 10. Momentum distributions of nucleons and α particles at $t = 150$ fm/c before the statistical decay in the reaction $^{12}\text{C} + ^{12}\text{C}$ at 45 MeV/nucleon with $b = 2$ fm. Results for the three sets 0.5σ , 1.0σ , and 1.5σ of the stochastic collision cross sections are shown.

The energy dependence and the σ dependence of the calculated flows of nucleons and fragments were found to be understandable, at least in the energy region where the flow is negative, by introducing the idea of two components of the collective flow. The first component is the flow of the dynamically emitted nucleons which are produced by stochastic collisions in the early stage of the reaction. Since the stochastic collisions erase the effect of the mean field, the flow of the dynamically emitted nucleons is small. The second component is the flow of the nuclear matter which contributes to the flows of fragments produced during the dynamical stage of the reaction. The flows of the evaporated nucleons and fragments inherit the flow of the parent fragments and hence the flows of dynamical fragments and the evaporated nucleons and fragments have almost common magnitude, common energy dependence, and σ dependence. Although the second component is affected largely by the mean field, its σ dependence is also large. However, this σ dependence turned out to come not from the change of

the flow angle but from change of the yield of the dissipated component in the momentum distribution of the fragments. Detailed comparison of the fragment momentum distribution with the data will be able to settle the in-medium cross sections. On the other hand, nucleon momentum distribution is mainly governed by the dynamically emitted nucleons in this energy region, and therefore the shape of the momentum distribution is not so sensitive to the in-medium cross sections.

We have mainly concentrated on the mechanism of the flow creation and the σ dependence in this paper, but the dependence on the effective interaction was not discussed in detail. What we have found is that the Gogny force is sufficient for the reproduction of the balance energy while the Volkov force fails. To calculate the flow with other effective interactions which reproduce the saturation property of the nuclear matter and have various incompressibilities is an important future problem for the determination of the equation of state of the nuclear matter.

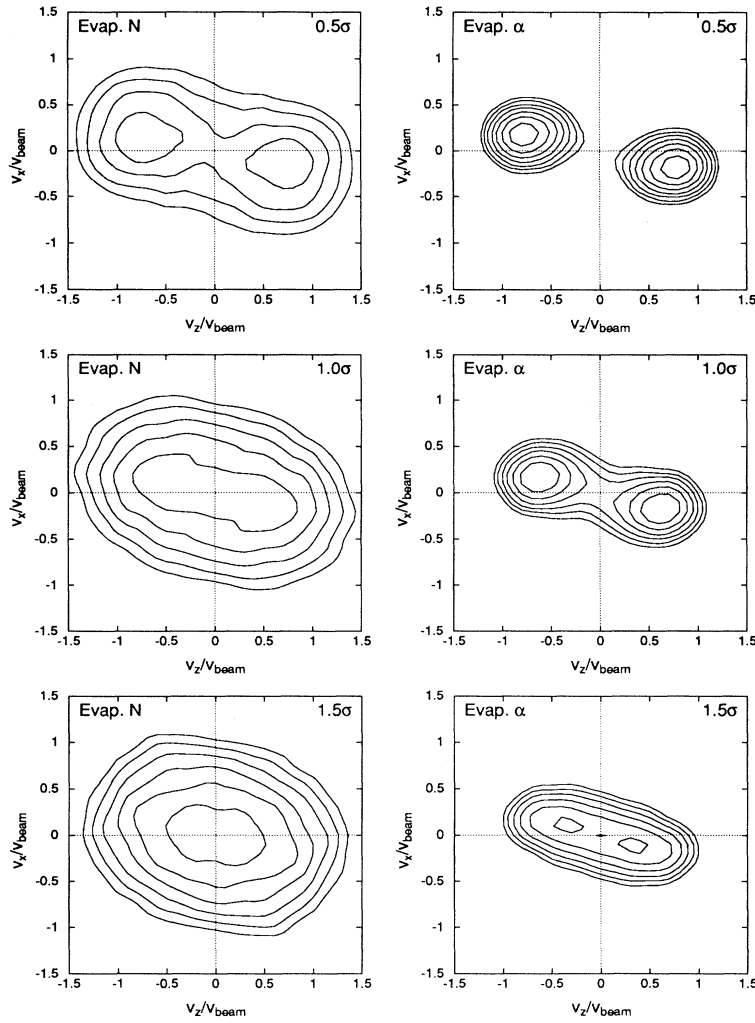


FIG. 11. The same as Fig. 10 but calculated from only the particles produced by the statistical decay.

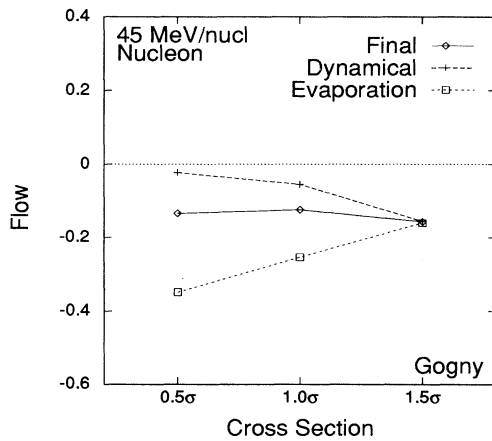


FIG. 12. Dependence of the flow of nucleons on the stochastic collision cross sections for the reaction $^{12}\text{C} + ^{12}\text{C}$ at 45 MeV/nucleon. The flow in this figure is defined as the slope of $\langle P_x \rangle - P_z$ curve at $P_z = 0$.

ACKNOWLEDGMENTS

The computational calculation for this work has been financially supported by Research Center for Nuclear Physics, Osaka University, as an RCNP Computational Nuclear Physics Project (Project No. 92-B-04).

APPENDIX A: DENSITY DEPENDENT INTERACTION

Here we consider an effective interaction which contains density dependent zero-range part,

$$V_\rho = \frac{t_\rho}{6} \sum_{i < j} X_{ij} \rho^\sigma(\mathbf{r}_i) \delta(\mathbf{r}_i - \mathbf{r}_j). \quad (\text{A1})$$

For example, the density dependent part of the Gogny force has this form with

$$t_\rho = 6t_3, \quad X = 1 + P_\sigma, \quad \sigma = 1/3. \quad (\text{A2})$$

By using the density $\rho(\mathbf{r})$ which is calculated from the

AMD wave function, the expectation value of V_ρ can be written as

$$\mathcal{V}_\rho = \langle V_\rho \rangle = \frac{t_\rho}{16} \int d\mathbf{r} \mu(\mathbf{r}) \rho^\sigma(\mathbf{r}), \quad (\text{A3})$$

where

$$\mu(\mathbf{r}) = \sum_\alpha \tilde{\rho}_\alpha(\mathbf{r}) \rho_\alpha(\mathbf{r}), \quad \rho(\mathbf{r}) = \sum_\alpha \rho_\alpha(\mathbf{r}), \quad (\text{A4})$$

$$\rho_\alpha(\mathbf{r}) = \left(\frac{2\nu}{\pi}\right)^{3/2} \sum_{i,j \in \alpha} e^{-2(\sqrt{\nu}\mathbf{r} - (\mathbf{Z}_i^* + \mathbf{Z}_j)/2)^2} B_{ij} B_{ji}^{-1}, \quad (\text{A5})$$

$$\tilde{\rho}_\alpha(\mathbf{r}) = \sum_\beta \frac{4}{3} \langle \alpha\beta | X | \alpha\beta - \beta\alpha \rangle \rho_\beta(\mathbf{r}). \quad (\text{A6})$$

Since the analytical integration of (A3) is impossible for noninteger σ and even in the case of $\sigma = 1$ the evaluation of the analytical sixfold summation is not feasible, we evaluate \mathcal{V}_ρ by the Monte Carlo method generating N_{TP} test particles randomly with an appropriate weight function $\mu_w(\mathbf{r})$,

$$\mathcal{V}_\rho \approx \frac{t_\rho}{16} \frac{F}{N_{\text{TP}}} \sum_{k=1}^{N_{\text{TP}}} \frac{\mu(\mathbf{r}_k)}{\mu_w(\mathbf{r}_k)} \rho^\sigma(\mathbf{r}_k), \quad F = \int d\mathbf{r} \mu_w(\mathbf{r}), \quad (\text{A7})$$

where \mathbf{r}_k is the position of the k th test particle. The arbitrary function $\mu_w(\mathbf{r})$ should be chosen so as to cover the important region in the integral (A3) efficiently and at the same time to make the generation of test particles numerically easy. By using the approximate density $\rho_w(\mathbf{r})$ calculated from the physical positions $\mathbf{R}_i = \text{ReW}_i$ as

$$\rho_w(\mathbf{r}) = \left(\frac{2\nu}{\pi}\right)^{3/2} \sum_i e^{-2(\sqrt{\nu}\mathbf{r} - \mathbf{R}_i)^2}, \quad (\text{A8})$$

we take $\mu_w(\mathbf{r})$ as

$$\mu_w(\mathbf{r}) = \rho_w(\mathbf{r})^2 = \left(\frac{2\nu}{\pi}\right)^3 \sum_{ij} e^{-(\mathbf{R}_i - \mathbf{R}_j)^2} e^{-4(\sqrt{\nu}\mathbf{r} - (\mathbf{R}_i + \mathbf{R}_j)/2)^2}, \quad (\text{A9})$$

$$F = \left(\frac{\nu}{\pi}\right)^{3/2} \sum_{ij} e^{-(\mathbf{R}_i - \mathbf{R}_j)^2}. \quad (\text{A10})$$

Derivatives of \mathcal{V}_ρ with respect to \mathbf{Z}_h are necessary to solve the equation of motion of AMD. They are also evaluated by the Monte Carlo method as

$$\frac{\partial \mathcal{V}_\rho}{\partial \mathbf{Z}_h^*} = \frac{t_\rho}{16} \int d\mathbf{r} \left[2\tilde{\rho}_\alpha(\mathbf{r}) + \frac{\sigma\mu(\mathbf{r})}{\rho(\mathbf{r})} \right] \rho^\sigma(\mathbf{r}) \frac{\partial \rho_\alpha(\mathbf{r})}{\partial \mathbf{Z}_h^*} \quad (\text{A11})$$

$$\approx \frac{t_\rho}{16} \frac{F}{N_{\text{TP}}} \sum_{k=1}^{N_{\text{TP}}} \left[2\tilde{\rho}_\alpha(\mathbf{r}_k) + \frac{\sigma\mu(\mathbf{r}_k)}{\rho(\mathbf{r}_k)} \right] \frac{\rho^\sigma(\mathbf{r}_k)}{\mu_w(\mathbf{r}_k)} \frac{\partial \rho_\alpha(\mathbf{r}_k)}{\partial \mathbf{Z}_h^*}, \quad (\text{A12})$$

where α is the spin-isospin label of the nucleon h .

APPENDIX B: DETAIL OF THE STOCHASTIC COLLISION PROCESS

In the higher energy region, we use the proton-neutron and proton-proton collision cross sections parametrized as

$$\sigma_{pn} = \max\left\{13335 E[\text{MeV}]^{-1.125}, 40\right\} \text{mb}, \quad (\text{B1})$$

$$\sigma_{pp} = \max\left\{4445 E[\text{MeV}]^{-1.125}, 25\right\} \text{mb}, \quad (\text{B2})$$

where E is the energy in the laboratory system of the stochastic collisions. These are based on the data of free cross sections. The neutron-neutron collision cross section is assumed to be identical to the proton-proton collision cross section. The nucleon-alpha collision total cross section $\sigma_{N\alpha,\text{tot}}$ is chosen to be equal to the total cross section of the process where the nucleon was scattered by two-nucleon collisions with four nucleons in the α cluster with the cross sections σ_{pn} and σ_{pp} . The adopted nucleon-alpha inelastic collision cross section is based on the experimental data parametrized [5] as

$$\sigma_{N\alpha,\text{inel}} = \max\left\{120 - 162e^{-(E-20 \text{ MeV})/(10 \text{ MeV})}, 0\right\} \text{mb}. \quad (\text{B3})$$

The angular distribution of proton-neutron scatterings are taken as

$$\frac{d\sigma_{pn}}{d\Omega} \propto 10^{-\alpha(\pi/2 - |\theta - \pi/2|)},$$

$$\alpha = \frac{2}{\pi} \max\left\{0.333 \ln E[\text{MeV}] - 1, 0\right\}, \quad (\text{B4})$$

while the proton-proton and neutron-neutron scatterings are assumed to be isotropic. The nucleon-alpha inelastic collision is treated as a two-nucleon collision between the nucleon and a nucleon in the α cluster and the same angular distribution as the two-nucleon collision is applied. The angular distribution of the nucleon-alpha elastic scattering is parametrized [5] as

$$\frac{d\sigma_{N\alpha,\text{el}}}{d\Omega} \propto \exp\left[-\left(\frac{180^\circ - \theta}{70^\circ}\right)^2\right] + 10 \exp\left[-\left(\frac{\theta - 20^\circ}{40^\circ}\right)^2\right]. \quad (\text{B5})$$

Since the above defined cross sections are too large if they are applied to a low energy region, we use the cross sections

$$\sigma_{pn} = \sigma_{pp} = \frac{100 \text{ mb}}{1 + E/(200 \text{ MeV}) + 2 \min\{(\rho/\rho_0)^{1/2}, 1\}}, \quad (\text{B6})$$

$$\sigma_{N\alpha,\text{tot}} = \frac{571 \text{ mb}}{1 + E/(200 \text{ MeV}) + 2 \min\{(\rho/\rho_0)^{1/2}, 1\}}, \quad (\text{B7})$$

which are similar to those we used in Ref. [5] for the reaction at 28.7 MeV/nucleon. The cross sections (B6) and (B7) are used if they are smaller than the cross sections σ_{pn} , σ_{pp} , and $\sigma_{N\alpha,\text{tot}}$ defined for the higher energy region by Eqs. (B1) and (B2). On the other hand, the same expressions of angular distributions and $\sigma_{N\alpha,\text{inel}}$ are used for the whole energy region.

APPENDIX C: SUBTRACTION OF SPURIOUS ZERO-POINT OSCILLATION

As in Refs. [3–5] the spurious kinetic energies of zero-point oscillations of center-of-mass motion of fragments are subtracted by modifying the Hamiltonian in the equation of motion of AMD as

$$\mathcal{H} = \langle H \rangle - \frac{3\hbar^2\nu}{2M}A + T_0(A - N_F), \quad (\text{C1})$$

where the zero-point kinetic energy T_0 is treated as a free parameter to adjust the gross feature of the binding energies of nuclei.

We define the fragment number N_F as

$$N_F = \sum_{i=1}^A \frac{g(k_i)}{n_i m_i}, \quad (\text{C2})$$

where

$$n_i = \sum_{j=1}^A \hat{f}_{ij}, \quad m_i = \sum_{j=1}^A \frac{1}{n_j} f_{ij}, \quad k_i = \sum_{j=1}^A \bar{f}_{ij} \quad (\text{C3})$$

and

$$\hat{f}_{ij} = F(d_{ij}, \hat{\xi}, \hat{a}), \quad f_{ij} = F(d_{ij}, \xi, a), \quad \bar{f}_{ij} = F(d_{ij}, \bar{\xi}, \bar{a}), \quad (\text{C4})$$

$$d_{ij} = |\text{Re}(\mathbf{Z}_i - \mathbf{Z}_j)|, \quad (\text{C5})$$

$$F(d, \xi, a) = \begin{cases} 1 & \text{if } d \leq a \\ e^{-\xi(d-a)^2} & \text{if } d > a \end{cases}. \quad (\text{C6})$$

TABLE I. Parameters concerned with the subtraction of spurious zero-point oscillations of fragments. Parameters which are used with the Gogny force in this paper are shown as well as those used with the Volkov force No. 1 with $m = 0.576$.

Force	ξ	a	$\hat{\xi}$	\hat{a}	$\bar{\xi}$	\bar{a}	g_0	σ	M	T_0
Volkov	1.0	0.2	2.0	0.1	—	—	—	—	—	7.7 MeV
Gogny	2.0	0.6	2.0	0.2	1.0	0.5	1.0	2.0	12.0	9.2 MeV

Compared to Ref. [3] where the Volkov force was used as the effective interaction, we have newly introduced a function

$$g(k) = 1 + g_0 e^{-(k-M)^2/2\sigma^2}, \quad (\text{C7})$$

which should be equal to 1 in principle. We have introduced it in order to remedy the situation that nuclei around ^{12}C are underbound while the binding energies of other nuclei such as α and ^{16}O are almost reproduced in the calculation with the Gogny force. We have chosen the parameters as shown in Table I. Binding energies of nuclei are sensitive only to two parameters, T_0 and M .

- [1] J. Péter, in *Proceedings of the International Symposium on Heavy Ion Physics and Its Application*, Lanzhou, 1990, edited by W. Q. Shen *et al.* (World Scientific, Singapore, 1991), p.191.
- [2] G. D. Westfall, W. Bauer, D. Craig, M. Cronqvist, E. Gualtieri, S. Hannuschke, D. Klakow, T. Li, T. Reposeur, A. M. Vander Molen, W. K. Wilson, J. S. Winfield, J. Yee, S. J. Yennello, R. Lacey, A. Elmaani, J. Lauret, A. Nadasen, and E. Norbeck, *Phys. Rev. Lett.* **71**, 1986 (1993).
- [3] A. Ono, H. Horiuchi, T. Maruyama, and A. Ohnishi, *Phys. Rev. Lett.* **68**, 2898 (1992).
- [4] A. Ono, H. Horiuchi, T. Maruyama, and A. Ohnishi, *Prog. Theor. Phys.* **87**, 1185 (1992).
- [5] A. Ono, H. Horiuchi, T. Maruyama, and A. Ohnishi, *Phys. Rev. C* **47**, 2652 (1993).
- [6] H. Feldmeier, *Nucl. Phys.* **A515**, 147 (1990).
- [7] H. Horiuchi, *Nucl. Phys.* **A522**, 257c (1991).
- [8] H. Horiuchi, T. Maruyama, A. Ohnishi, and S. Yamaguchi, in *Proceedings of the International Conference on Nuclear and Atomic Clusters*, Turku, 1991, edited by

- M. Brenner, T. Lönnroth, and F. B. Malik, (Springer, Berlin, 1992), p. 512; in *Proceedings of the International Symposium on Structure and Reactions of Unstable Nuclei*, Niigata, 1991, edited by K. Ikeda and Y. Suzuki (World Scientific, Singapore, 1992), p.108.
- [9] J. Dechargé and D. Gogny, *Phys. Rev. C* **43**, 1568 (1980).
- [10] T. Maruyama, A. Ono, A. Ohnishi, and H. Horiuchi, *Prog. Theor. Phys.* **87**, 1367 (1992).
- [11] F. Pühlhofer, *Nucl. Phys.* **A280**, 267 (1977).
- [12] A. Volkov, *Nucl. Phys.* **75**, 33 (1965).
- [13] F. Sébille, G. Royer, C. Grégoire, B. Remaud, and P. Schuck, *Nucl. Phys.* **A501**, 137 (1989).
- [14] J. Aichelin, *Phys. Rep.* **202**, 233 (1991).
- [15] N. Brummund, thesis, University of Münster.
- [16] D. Klakow, G. Welke, and W. Bauer, Report No. MSUCL-884, WSU-NP-93-1 (unpublished); in *Proceedings of the 8th Winter Workshop on Nuclear Dynamics*, Jackson Hole, 1992, edited by W. Bauer and B. Back (World Scientific, Singapore, 1992), p. 190.
- [17] A. Ono, H. Horiuchi, and T. Maruyama, RCNP annual report, 1992.